

Taxonomy-Aware Continual Semantic Segmentation in Hyperbolic Spaces for Open-World Perception

Julia Hindel, Daniele Cattaneo, and Abhinav Valada

Abstract—Semantic segmentation models are typically trained on a fixed set of classes, limiting their applicability in open-world scenarios. Class-incremental semantic segmentation aims to update models with emerging new classes while preventing catastrophic forgetting of previously learned ones. However, existing methods impose strict rigidity on old classes, reducing their effectiveness in learning new incremental classes. In this work, we propose **Taxonomy-Oriented Poincaré-regularized Incremental-Class Segmentation (TOPICS)** that learns feature embeddings in hyperbolic space following explicit taxonomy-tree structures. This supervision provides plasticity for old classes, updating ancestors based on new classes while integrating new classes at fitting positions. Additionally, we maintain implicit class relational constraints on the geometric basis of the Poincaré ball. This ensures that the latent space can continuously adapt to new constraints while maintaining a robust structure to combat catastrophic forgetting. We also establish eight realistic incremental learning protocols for autonomous driving scenarios, where novel classes can originate from known classes or the background. Extensive evaluations of TOPICS on the Cityscapes and Mapillary Vistas 2.0 benchmarks demonstrate that it achieves state-of-the-art performance. We make the code and trained models publicly available at <http://topics.cs.uni-freiburg.de>.

I. INTRODUCTION

Automated vehicles rely on scene semantics predicted from online sensor data [1] as well as HD maps [2] for safe navigation. The dominant paradigm for scene understanding exploits semantic [3] or panoptic segmentation models [4] trained on a dataset with a fixed number of predetermined semantic categories. However, such vehicles operate in an open-world scenario where training data with new object classes appear over time. While one line of research focuses on detecting unknown objects [5], Class-Incremental Learning (CIL) aims to update the model with new classes at periodic timesteps [6]. On one hand, training a new model from scratch every time new classes appear is not only computationally inefficient but also requires past and present data to be available. On the other hand, simply updating a trained model with new data will result in catastrophic forgetting of old knowledge as the model will be biased towards new classes [7]. Consequently, CIL methods aim to balance observing characteristics of new classes while preserving patterns of formerly learned classes as the model is evaluated on all seen classes [6].

Class-Incremental Semantic Segmentation (CISS) incorporates the background shift as an additional challenge. This phenomenon occurs as pixels that belong to old classes are labeled

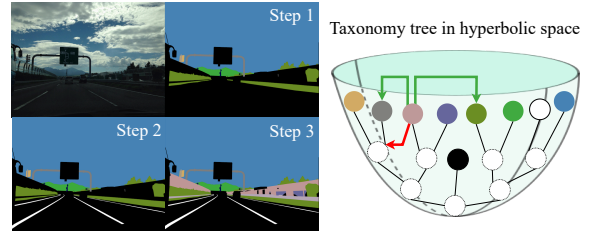


Fig. 1: TOPICS leverages the explicit class taxonomy (black) and implicit relations (red and green) in hyperbolic space to balance rigidity and plasticity in taxonomic class-incremental semantic segmentation.

as background in new data samples [8]. Consequently, CISS methods need to address label inconsistencies, catastrophic forgetting, and generalization on new classes at the same time. State-of-the-art CISS methods restrain the forgetting of old knowledge with data replay, network expansion, or regularization. The latter focuses on constraining features of the new model to imitate those of the prior model with direct feature distillation [9] or frozen old class weights [10], [11]. We find that these restrictions significantly hinder the plasticity of the model as old class features cannot evolve.

Furthermore, most methods are tailored to the highly curated PascalVOC dataset which deviates significantly from densely annotated automated driving scenarios. While two to three object categories appear per image in PascalVOC, driving datasets typically contain over twenty different object categories, and fewer pixels are assigned to the background class. Additionally, all CISS methods assume that new classes originate from the prior background. This scenario is unrealistic for automated driving as a change in requirements for navigation could also entail bifurcations of previously observed classes for better decision-making, e.g. a model is initially trained to uniformly segment humans but later this ability needs to be extended to distinguish different vulnerable road users.

In this work, we introduce taxonomy-aware continual semantic segmentation for automated driving scenarios. Our proposed *Taxonomy-Oriented Poincaré-regularized Incremental Class Segmentation (TOPICS)* approach enforces features conform to taxonomy-tree structures in hyperbolic space. As a result, the overall class distribution is rigid and new classes are appended at fitting positions in Fig. 1. This supervision also provides plasticity for old classes as the positions of ancestors are updated according to new classes. We show that this regularization is beneficial for open-world scenarios since it includes aspects of plasticity and rigidity. To further avoid catastrophic forgetting, we incorporate pseudo-labeling of the background and relation constraints of old class hyperplanes

in TOPICS. We argue that semantic classes inherit relations that go beyond the defined class taxonomy such as similar appearances or contexts. Those relations can be observed as close mappings in latent space. We ensure consistency of the relations between prior class hyperplanes to increase the rigidity of our model. Lastly, we constrain features to have equidistant radii to maintain constant scarcity. We ensure that prior class features can only move in a circular direction around the hyperbolic center. Accordingly, new classes cannot result in a latent space shift of the complete taxonomy in their favor. We perform extensive evaluations of TOPICS on the standard Cityscapes [12] and Mapillary Vistas 2.0 [13] benchmarks where it sets the new state-of-the-art.

Our main contributions can thus be summarized as follows:

- TOPICS, a taxonomic-aware modeling in hyperbolic space to balance plasticity and rigidity for CISS.
- Two novel regularization losses tailored for incremental learning in hyperbolic space.
- Extensive evaluations and ablation study under eight different universal CISS settings for autonomous driving.
- Publicly available code and pretrained models at <http://topics.cs.uni-freiburg.de>.

II. RELATED WORK

In this section, we summarize existing works in class-incremental semantic segmentation, hyperbolic neural networks, and hierarchical learning.

Class-Incremental Semantic Segmentation: CISS methods rely on data replay, expansion, or distillation to avoid catastrophic forgetting. Prior data is recreated with GANs [14] or a small subset of prior data is stored in memory-buffers [11]. To further reduce memory constraints, prior work stores selected feature representations instead of raw data [15]. Expansion-based methods dedicate separate network components for particular semantic knowledge. For example, one branch of parallel convolutions adapts to the new data and is merged into the frozen branch after every incremental step [16]. Follow-up work extends this idea by fusing only endpoints of a trainable and frozen model in combination with distillation [17]. Distillation approaches maintain prior model weights to restrain the current model for equivalent responses to the input data [6]. The pioneering approach MiB [8] relates prior background logits to the combination of novel-class and background logits in the new model. This method is enhanced with gradient-based attribution weight initialization which identifies relevant classifier weights for novel classes from prior weights of the background class [18]. On the other hand, PLOP [9] labels the background with prior model predictions and distills pooled intermediate feature representations. Subsequent work focuses on learning an enhanced weighting term for distillation [19] or adapting this principle to transformer architectures [7], [20]. The method SATS [20] also highlights the benefit of relation distillation between self-attention vectors in a SegFormer model. This weaker constraint allows the model to avoid forgetting while not constraining its plasticity. Prior work also trains segmentation models with sigmoid activation and binary

cross-entropy loss as the instability of softmax activations hinders incremental learning [11]. DKD [21] further combines this approach with decoupled knowledge distillation while other approaches completely freeze the feature extractor and segment unknown background classes with saliency detectors [11] or pre-trained models [10].

However, all observed methods focus on novel classes from the background which significantly hinders their applicability in real-world scenarios where incremental learning could also entail a refinement of known classes. In this paper, we propose to simultaneously benchmark CISS methods for incremental learning from known classes and the background in the context of autonomous driving. Further, CISS methods do not utilize semantic relationships between classes to balance plasticity and rigidity. We hypothesize that a hierarchical mapping of class features facilitates learning new classes while it constrains forgetting old classes.

Hyperbolic Neural Networks: Hyperbolic neural networks have been first proposed to capture tree-like structures in text and graphs. For CNNs, the hyperbolic classification is modeled as a prototype-based approach [22], [23] or multinomial logistic regression as proposed by [24]. For the first, a cone entailment loss enforces all descendant prototypes to lie in the same geometric cone [25]. In multinomial logistic regression, semantic classes are geometrically interpreted as hyperplanes, and hierarchies are explicitly modeled with a hierarchical softmax [26] or cosine margins [27]. While hyperbolic neural networks have been extensively explored in image classification [27], [28] and metric learning [25], few prior works focus on semantic segmentation. Atigh *et al.* [26] first shows the potential of applying hyperbolic multinomial regression for image segmentation. Follow-up work highlights the dense calibration capabilities of this network [29] and leverages it for active learning [30]. One pioneering work also explores hyperbolic spaces for class-incremental image classification and highlights the positive impact of geometric-induced clear decision boundaries [23]. Motivated by them, our work is the first to explore hyperbolic spaces for CISS.

Hierarchical Learning: Hierarchical segmentation methods outperform flat classifiers on leaf categories by modeling the semantic hierarchy of classes in features [31] or combining logits with those of ancestor classes [26], [32]. While hierarchical semantic segmentation primarily addresses closed class settings, prior work in image classification concentrates on taxonomic class-incremental learning with network expansion [31] and replay-buffers [33]. Lin *et al.* first focused on taxonomic incremental semantic segmentation [33]. However, they require all ancestor classes to be present in the base training and allow the usage of all history data which contradicts CISS principles. We introduce a more realistic form of taxonomic class-incremental semantic segmentation which allows increments from both background and known classes and complies with other CISS task definitions.

III. TECHNICAL APPROACH

In this section, we first introduce taxonomic CISS. We then present our TOPICS approach which is tailored to

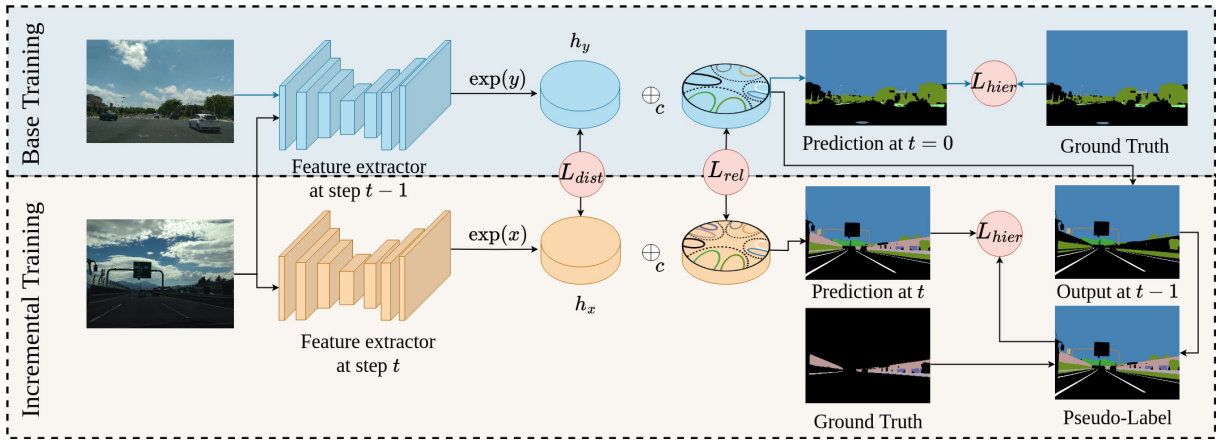


Fig. 2: During base training of TOPICS, features are mapped onto the Poincaré ball before the class hierarchy is explicitly enforced with \mathcal{L}_{hier} . In incremental steps, the old model is used to generate pseudo-labels of old classes and to regularize the last layer’s weights with \mathcal{L}_{rel} and feature radii with \mathcal{L}_{dist} .

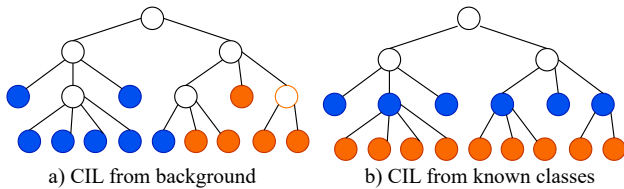


Fig. 3: Visualization of the class taxonomic tree \mathcal{H} : a) Novel classes originate from the background and b) Novel classes originate from known classes. Base classes (\mathcal{C}^1) are colored in blue whereas novel classes ($\mathcal{C}^{2:T}$) are colored in orange. Novel ancestor nodes are visualized with orange outlines.

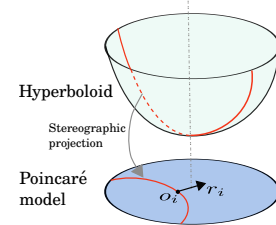


Fig. 4: Visualization of a hyperplane on an upper sheet of a two-sheeted hyperboloid which is projected on a 2D Poincaré ball. The hyperplane has an offset of o_i from the center and an orientation r_i .

incrementally learn new classes from either background or prior known classes as shown in Fig. 2. We leverage the class taxonomy and implicit relations between prior classes to avoid catastrophic forgetting in incremental learning steps. We first train the model on the base dataset. The class hierarchy is explicitly enforced in the final network layer which is mapped in hyperbolic space. This geometric space ensures that classes are equidistant to each other irrespective of their hierarchy level which facilitates learning tree-like class hierarchy structure. During the incremental steps, we leverage the old model’s weights to create pseudo-labels for the background and employ scarcity and relation-regularization losses to maintain important relations of old classes while learning the novel classes in a supervised manner.

A. Class-Incremental Semantic Segmentation

CISS aims at training a model f_θ over $t = 1, \dots, T$ incremental tasks. The first task ($t = 1$) is denoted as base training while all subsequent tasks $t = 2, \dots, T$ are referred to as incremental steps. Every task is defined by its own disjoint label space \mathcal{C}^t and training dataset $(x^t, y^t) \in \mathcal{D}^t$. x^t refers to task-specific input images and $y^t \in \mathcal{Y}^t$ their pixelwise label according to $\mathcal{Y}^t = b^t \cup \mathcal{C}^t$. The background class b^t includes all pixels whose true semantic class (y) is not included in \mathcal{C}^t . We consider the more realistic overlapped setting of CISS where training images (x^t) may include pixels whose dataset ground truth labels are old, current, or future classes. Their corresponding training label (y^t) is re-defined according to \mathcal{Y}^t . After every task t , the network is challenged to make predictions on $\mathcal{C}^{1:t}$ whereas only true background pixels

should not be associated with a semantic class.

In comparison to [8]–[11], [21], we do not constrain future classes to originate from the background in taxonomic CISS. We regard incremental scenarios where future classes are refinements of known classes or the background as shown in Fig. 3. We define $\mathcal{C}^{1:T}$ according to a class taxonomy tree \mathcal{H} which has l hierarchy levels and N_L leaf nodes. Unlike taxonomic CIL as defined in [31], we allow unbalanced trees and ancestor nodes to be introduced when its first leaf node N_{L_i} is observed as illustrated in Fig. 3a. Consequently, we generate more realistic incremental learning scenarios which are not restricted to breadth-first increments. When classes are refined from known classes (Fig. 3b), we define disjoint subsets \mathcal{D}^t according to a fixed ratio, i.e. \mathcal{Y}^t of every x_i is constant and the same image cannot be observed with different labeling taxonomies at different time steps.

B. Semantic Segmentation with the Poincaré Model

We model the class hierarchy in hyperbolic space due to its favorable property of equidistant node connections on all hierarchy levels. Consequently, distances are inversely proportional to the semantic similarity of classes. The hyperbolic space follows the geometry of constant negative curvature which is defined in the variable c . The Poincaré model is a stereographic projection of the upper sheet of a two-sheeted hyperboloid and is, therefore, represented by a unit ball as shown in Fig. 4. This hyperbolic model is formally defined by the manifold $\mathbb{D}_c^n = \{x \in \mathbb{R}^n : c\|x\| < 1\}$ and

Riemannian metric

$$g^{\mathbb{D}_c^N} = (\lambda_x^c)^2 g^{\mathbb{E}} = \left(\frac{2}{1 - c\|x\|^2} \right)^2 g^{\mathbb{E}}, \quad (1)$$

where $g^{\mathbb{E}}$ is the euclidean tensor and λ_x^c the conformal factor. When $c = 0$, the Euclidean geometry is recovered.

For our TOPICS model, we only map the last neural network layer to hyperbolic space. Therefore, we first project the Euclidean features e on the Poincaré ball at its origin which is defined as

$$h_i = \exp_0(e_i) = \tanh(\sqrt{c}\|e_i\|)(e_i/(\sqrt{c}\|e_i\|)). \quad (2)$$

The geometric interpretation of multinomial regression in hyperbolic space suggests that every class y is represented as a hyperplane in the Poincaré ball with offset $o_y \in \mathbb{D}_c^N$ and orientation $r_y \in T\mathbb{D}_c^N$ (Fig. 4)

$$H_y^c = \{h_i \in \mathbb{D}_c^N, \langle -o_y \oplus_c h_i, r_y \rangle = 0\}. \quad (3)$$

Consequently, the likelihood of a class is defined as

$$p(\hat{y} = y | h_i) \propto \exp(\zeta_y(h_i)), \quad (4)$$

where ζ_y is the signed distance of the feature h_i to the hyperplane of y which is approximated according to

$$\zeta_y(h_i) = \frac{\lambda_{o_y}^c \|r_y\|}{\sqrt{c}} \sinh^{-1} \left(\frac{2\sqrt{c} \langle -o_y \oplus_c h_i, r_y \rangle}{(1 - c\| -o_y \oplus_c h_i \|^2) \|r_y\|} \right) \quad (5)$$

with \oplus_c being the Möbius addition

$$v \oplus_c w = \frac{(1 + 2c\langle v, w \rangle + c\|w\|^2)v + (1 - c\|v\|^2)w}{1 + 2c\langle v, w \rangle + c^2\|v\|^2\|w\|^2}. \quad (6)$$

C. Hierarchical Segmentation

We model the hierarchy of semantic classes in the last layer of the network. We opt for a binary cross-entropy loss to ensure magnitudes of old and new class predictions do not correlate. Specifically, we extend the state-of-the-art hierarchical segmentation loss [32] to multi-hierarchy levels and show its beneficial impact for incremental learning in hyperbolic space. Therefore, we model leaf nodes and all their ancestors as separate output classes \mathcal{V} and use a combination of ancestor \mathcal{A} and descendant \mathcal{D} logits (s) in the loss function. We follow the tree-min loss [32] defined as

$$\mathcal{L}_{TM} = \sum_{v \in \mathcal{V}} -l \log \left(\min_{u \in \mathcal{A}_v} (s_u) \right) - (1 - l) \log \left(1 - \max_{u \in \mathcal{D}_v} (s_u) \right), \quad (7)$$

which penalizes hierarchical-inconsistent predictions for every class. For a correct prediction l , this loss penalizes the smallest logit of its ancestors \mathcal{A}_v . On the other hand, for wrong predictions $1 - l$, \mathcal{L}^{TM} punishes the maximum logits of its descendant \mathcal{D}_v to reduce the score of complete root-to-leaf branches.

Further, we separately employ a categorical cross-entropy (\mathcal{L}_{CE}) on every hierarchy level. Therefore, we first retrieve $s'_v = \max_{u \in \mathcal{D}_v} (s_u)$ and convert the labels y_t into unique binary labels for every hierarchy level l . This loss penalizes

high prediction scores of sibling class descendants. The complete hierarchical loss is defined as

$$\mathcal{L}_{hier} = \alpha \mathcal{L}_{TM} + \beta \mathcal{L}_{CE}. \quad (8)$$

During inference, we multiply the logits of every leaf node v_L with the logits of all its ancestors (\mathcal{A}_{v_L}) and remove non-leaf classes from the evaluation.

D. Hierarchical Relation Distillation

We reason that apart from explicit taxonomy relations between classes, an image model also captures implicit relations between classes in the form of relative similarity in feature space. Therefore, we aim to constrain these implicit relations to maintain relevant old class knowledge. In line with [20], [34], we argue that distilling relations is preferable to direct feature distillation as the latter restricts the model from re-distributing the feature space according to new classes. In comparison to the named prior work which distills relations based on feature maps, we propose to regularize the last layer's weights with this constraint. Consequently, we employ an InfoNCE loss on the hyperbolic class hyperplanes \mathcal{H}_t to maintain closely grouped classes of the prior model in a similar constellation in the updated model. We define a distance between two classes y^1 and y^2 as the distance between one class offset o_{y^1} and the hyperplane of the other class H_{y^2} .

As outlined in Sec. III-B, an offset o_{y^1} is a vector in hyperbolic space which defines the hyperplane of a class y^1 with orientation r_{y^1} . We retrieve absolute distances $d_{y^1}^{y^2}$ from signed distances which are computed using $\zeta_{y^2}(o_{y^1})$ as defined in Eq. (5). Before beginning the training procedure, we utilize the old model's weights to compute the top k most similar hyperplanes H_y for every offset o_y in $\mathcal{C}^{1:t-1}$. We neglect the background class in computing distances as we do not want to make constraints based on this variable class. Further, we denote all positive anchors of a class, $k_{y^1}^+$, as the top k smallest absolute distances to o_{y^1} and enforce these relations to be maintained during the incremental training. We apply an InfoNCE-inspired loss:

$$\mathcal{L}_{rel} = -\log \frac{\exp(1 - \tau \cdot d_{k^+}/d_{max})}{\sum_{i=0}^D \exp(1 - \tau \cdot d_i/d_{max})}. \quad (9)$$

with τ being the temperature hyper-parameter. With this constraint, we ensure relative implicit relations between old classes are maintained which creates an additional supervision for prior classes $\mathcal{C}^{1:t-1}$.

E. Hyperbolic Distance Correlation

Prior research highlights the correlation of the hyperbolic radius to the scarcity of observed features [30] or the uncertainty of predictions in low dimensional space [26]. As incremental data is unbalanced with new classes appearing more frequently, we aim to constrain the radii of features to be unchanged between the old and new models. Therefore, we enforce features of the new and old model to be equidistant from the center of the Poincaré ball. We hypothesize that this constraint results in the hyperplanes of old classes rotating around the center and prevents a shift of the complete

taxonomic tree in favor of the new classes. New space is allocated for new classes while the respective scarcity of old classes is not affected.

IV. EXPERIMENTAL EVALUATION

In this section, we present quantitative and qualitative results of TOPICS on nine CISS settings in addition to a comprehensive ablation study to underline the importance of our contributions. Further, we detail the applied CISS settings and the training protocol that we employ.

A. Datasets

We evaluate TOPICS on the Cityscapes [12] and Mapillary Vistas 2.0 [13] datasets. For both datasets, we define CISS protocols where incremental classes either primarily originate from the background or known classes. We only consider the more realistic case of overlapped CISS where image pixels can belong to old, current, or future classes at any timestep. The Cityscapes dataset consists of 19 semantic classes in addition to a void class. For CISS from the background, we adapt the 14-1 (6 tasks) and 10-1 (10 tasks) setting as proposed in [18]. The first 10 or 14 classes are learned during base training while one class is added per incremental step. The task count includes base training as the first task. For CISS from known classes, we learn 7 base classes that correspond to the official sub-categories defined for Cityscapes and increment the model in a 7-4 (4 tasks) or 7-18 (2 tasks) manner.

For Mapillary Vistas 2.0, we leverage 111 valid semantic classes and collapse all void pixels into one background class. Consequently, we define the settings of 51-30 (3 tasks), and 71-10 (5 tasks) for CISS from the background. On the other hand, we evaluate taxonomic incremental capabilities with 39-84 (2 tasks) and 39-21 (5 tasks) on this dataset. For both datasets, we use the official validation split for testing and split the training data into training vs. validation with an 80:20 ratio. We note that the validation and test data remain constant for all incremental steps. For CISS from known classes, we divide the dataset into base and incremental dataset splits according to the number of learned classes within each step.

B. Experimental Setup

In line with prior work [8]–[10], we use the DeepLabV3 model with the ResNet-101 backbone which is pre-trained on ImageNet for all the experiments. We employ the Geopt library [35] to project the Euclidean features to a Poincaré ball with $c = 2.0$ (different curvatures are explored in Sec. IV-D.5). Further, we follow the Möbius approximation defined in [26] for more efficient computations. We train TOPICS for 60 epochs per task with batch size 24 for Cityscapes and 16 for Mapillary Vistas 2.0 using the Riemannian SGD optimizer with momentum of 0.9 and weight decay of 0.0001. We use a poly learning rate scheduler with initial learning rates of 0.05 for base training and 0.01 in all incremental steps. We additionally ablate lower learning rates in Sec. IV-D.2. For the hierarchical loss function, we set the hyper-parameters to $\alpha = 5$ and $\beta = 1$ and ablate different hierarchical functions in Sec. IV-D.4. For Mapillary Vistas 2.0, we rescale the longest size to 2177 pixels before taking a non-empty crop

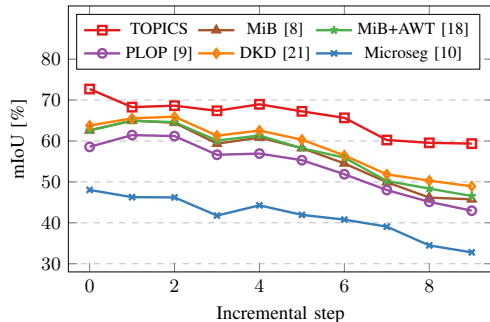


Fig. 5: Performance at every increment on Cityscapes 10-1 (10 task) setting.

of (1024,1024) and horizontal flipping. On the other hand, we train on random non-empty crops of (512,1024) with horizontal flipping for Cityscapes. Non-empty cropping biases image crops to include labeled masks (i.e. new classes) which could be neglected when applying random cropping.

C. Quantitative Results

We compare TOPICS with five state-of-the-art CISS methods: PLOP [9], MiB [8], MiB+AWT [18], DKD [21] and MicroSeg [10]. For each method, we use the respective author’s published code and use the same augmentations outlined in Sec. IV-B. For Cityscapes, we train the method PLOP on 512×512 crops as the method is restricted to squared input images. We evaluate the models using the mean intersection-over-union (mIoU) metric. Specifically, we evaluate the mIoU over all the base classes (\mathcal{C}_1) and novel classes ($\mathcal{C}_{2:T}$) separately as an indication of rigidity and plasticity. We present the results on Cityscapes in Tab. I. On this dataset, TOPICS outperforms all baselines by at least 9.88pp on the CISS from the background. While the difference in base IoU measures 4.2pp, our method significantly exceeds the benchmarks by at least 16.9pp in terms of novel IoU. This finding emphasizes that a balance between plasticity and rigidity is crucial to achieving superior results for class incremental learning. Further, we note the largest performance difference on incremental scenarios from known classes where TOPICS exceeds the best baseline by 29.94pp in mIoU. Consequently, we highlight the versatility of our method to balance plasticity and rigidity in all tested CISS settings. DKD [21] achieves the highest benchmark on CISS from the background in our setting but does not generalize on the bifurcation of previously observed classes which we reason with frozen layers in incremental steps. The MicroSeg approach also does not result in a favorable performance on Cityscapes and Mapillary Vistas 2.0 which is caused by low-quality proposals retrieved from the COCO dataset in addition to fully freezing the backbone. Subsequently, we present the mIoU over different increments for the 10-1(10 tasks) scenario on Cityscapes in Fig. 5. We note that for most benchmarks the mIoU increasingly deteriorates after incremental step 3. On the other hand, TOPICS achieves a constant performance from step 1 to step 6 after which the performance again stabilizes. Therefore, our approach supremely maintains base as well as incremental class knowledge while not restricting the adaptability to new classes.

TABLE I: Continual semantic segmentation results on Cityscapes in mIoU (%). Tasks defined as $\mathcal{C}^1\text{-}\mathcal{C}^T$ (T tasks) and h class hierarchy increments.

Method	14-1 (6 tasks)			10-1 (10 tasks)			7-4 (4 tasks)h			7-18 (2 tasks)h		
	1-14	15-19	all	1-10	11-19	all	1-7	8-25	all	1-7	8-25	all
PLOP [9]	63.54	15.38	48.33	60.75	27.97	42.96	88.56	18.14	20.75	88.73	15.06	17.99
MiB [8]	66.37	14.36	50.05	61.80	32.97	45.73	77.66	6.61	9.83	90.10	5.71	9.64
MiB + AWT [18]	65.60	19.19	50.72	60.97	35.70	46.55	84.65	10.46	13.64	90.19	5.61	9.56
DKD [21]	68.83	14.70	51.86	66.77	34.52	48.92	89.46	0.56	4.98	89.19	4.29	8.32
MicroSeg [10]	51.35	11.61	38.84	44.37	23.55	32.78	86.39	1.63	5.79	86.37	7.71	11.26
TOPICS (Ours)	73.03	42.47	61.74	71.37	52.62	59.36	90.02	51.31	50.69	90.33	61.62	59.98

TABLE II: Continual semantic segmentation results on Mapillary Vistas 2.0 in mIoU (%). Tasks defined as $\mathcal{C}^1\text{-}\mathcal{C}^T$ (T tasks) and h class hierarchy increments.

Method	51-30 (3 tasks)			71-10 (5 tasks)			39-84 (2 tasks)h			39-21 (5 tasks)h		
	1-51	52-111	all	1-71	72-111	all	1-39	40-123	all	1-39	40-123	all
PLOP [9]	20.83	8.97	14.59	18.12	5.74	13.83	19.15	5.52	9.51	17.79	3.14	6.64
MiB [8]	16.72	11.48	13.77	15.10	8.43	12.58	19.38	13.61	11.64	16.49	6.51	8.86
MiB + AWT [18]	18.33	13.27	15.89	15.78	9.69	13.91	19.76	13.47	15.47	17.75	11.16	12.84
DKD [21]	25.49	12.82	18.74	22.71	11.03	18.65	24.24	3.20	9.15	28.04	1.53	8.06
MicroSeg [10]	9.39	4.19	6.62	8.38	3.46	6.65	12.70	1.07	4.41	13.69	0.80	4.08
TOPICS (Ours)	23.76	17.78	20.35	22.10	14.55	19.20	24.16	21.49	21.94	26.67	22.57	23.35

We present the results on Mapillary Vistas 2.0 in Tab. II. TOPICS outperforms all baselines by at least 1.6pp on all CISS benchmarks. We justify these results with the rigidity of our model towards base classes while not restraining the learning of new knowledge. Our method significantly outperforms the baselines on novel IoU where we record an improvement of at least 3.5pp. Further, the baselines significantly underperform on the CISS from known classes setting which shows the need for solutions tailored for both scenarios. We observe that TOPICS seemingly integrated the CISS from known classes into its hierarchical learning paradigm. We further discuss the performance on base classes in the supplementary material Sec. S.1.

D. Ablation Study

In this section, we analyze the impact of various architectural components and hyperparameters on the performance of our approach. We perform all the ablation experiments on the Cityscapes 14-1 (6 tasks) setting.

1) *Influence of Different Components:* We show in Tab. III that hyperbolic spaces are better calibrated and a mapping of the final layer to this space increases the performance after base training by 0.79pp which complements findings in [29]. Further, the performance improvement increases to 2.52pp in mIoU after the final step which can be attributed to a difference of 5.73pp in novel classes. Consequently, we suggest that equidistant class mappings in hyperbolic space support incremental learning. Further, we find that our hierarchical loss results in a performance improvement of 1.85pp which can be attributed to a performance increase in base and novel classes. Base classes benefit from the rigidity of the feature space as well as a high quality of learned features in base training (1.34pp in comparison to the flat classifier) which helps prevent forgetting [36]. Additionally, the generalization on new classes is amplified by 6.52pp. We reason that learning new classes is eased in a hierarchy as their mapping is already defined by trained ancestor nodes. Consequently, we motivate hierarchical modeling in neural

TABLE III: Ablation study on the efficacy of various components of TOPICS. All results are reported on Cityscapes in mIoU (%). The setting $1 - 14_0$ represents the mIoU on base classes at time $t = 0$.

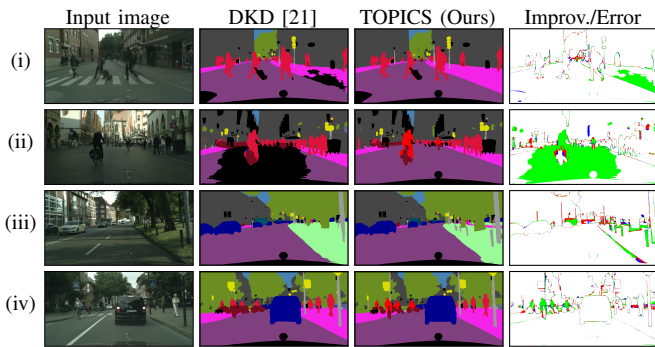
Space	14-1 (6 tasks)						
	\mathcal{L}_{hier}	\mathcal{L}_{dist}	\mathcal{L}_{rel}	1-14 ₀	1-14	15-19	all
Eucl.				72.72	71.06	29.09	57.02
Hyperb.				73.51	72.62	34.82	59.54
	✓			74.85	72.94	41.34	61.39
	✓	✓		74.85	72.98	42.06	61.60
	✓	✓	✓	74.85	73.03	42.47	61.74

TABLE IV: Influence of different learning rates and number of epochs during training increments on Cityscapes in mIoU (%).

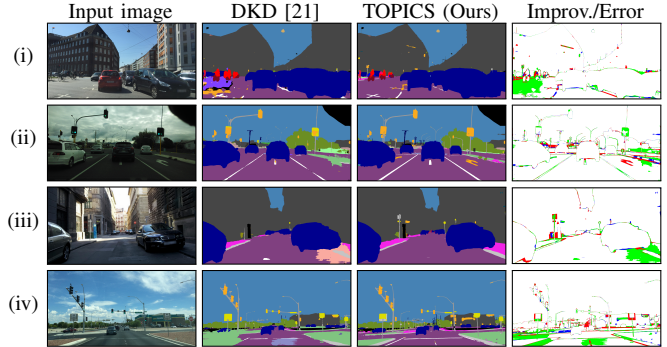
		14-1 (6 tasks)		
Learning Rate	Epochs	1-14	15-19	all
0.001	30	71.72	21.07	55.47
0.001	60	72.72	27.43	57.76
0.01	30	73.19	28.74	58.42
0.01	60	73.03	42.47	61.74

networks for open-world learning. Our regularization losses increase the performance by 0.21pp and 0.14pp, respectively. We note that newly added classes significantly benefit from our constant sparsity constraint (0.73pp) as their relative frequency largely differs in subsequent incremental steps. Further, constraining implicit class relations further improves the knowledge retention of new classes by 0.41pp.

2) *Learning Rate and Epochs:* Some benchmarks adopt a lower learning rate [8], [9], [18], [21] and train for less epochs [8], [9], [18] during incremental steps. While our model benefits from the selected settings, we additionally show in Tab. IV that TOPICS also outperforms all benchmarks with their selected hyperparameters. We note that training our model for shorter epochs or a lower learning rate significantly decreases the generalization on novel classes ($\mathcal{C}_{1:T}$). Further, the performance on base classes is affected which we reason with false positive segmentation of base classes. When training for 30 epochs on a learning rate of 0.01 this effect seems diminished as the base performance peaks with this reduced number of iterations.



(a) Semantic segmentation results on Cityscapes 10-1 (10 tasks).



(b) Semantic segmentation results on Mapillary Vistas 2.0 71-10 (5tasks).

Fig. 6: Qualitative results of TOPICS in comparison to the best performing baselines for CISS on the Cityscapes and Mapillary Vistas 2.0 dataset. The improvement/error maps show pixels misclassified by the baseline and correctly predicted by TOPICS in green and vice-versa in blue. Incorrect predictions of both models are colored in red.

TABLE V: Influence of regularisation weighting term for results on Cityscapes in mIoU (%).

\mathcal{L}_{dist}	\mathcal{L}_{rel}	14-1 (6 tasks)		
		1-14	15-19	all
0.001	10	72.92	42.64	61.70
0.1	10	73.10	42.21	61.72
0.01	10	73.03	42.47	61.74
0.01	1	73.05	42.08	61.65
0.01	100	73.08	41.29	61.48

TABLE VI: Influence of different hierarchical loss functions for results on Cityscapes in mIoU (%).

Hierarchical Loss Function	14-1 (6 tasks)		
	1-14	15-19	all
Hierarchical BCE	60.72	22.06	48.02
Tree-min	73.03	42.47	61.74
Tree-min + Margin loss [32]	72.97	35.31	59.91

3) *Weighting of Loss Functions*: We ablate the weighting of our hierarchical relation distillation loss and hyperbolic distance correlation loss in Tab. V. We note that a higher weighting of either loss increases the rigidity of the model which can be observed as higher base class scores. As a result, the plasticity is negatively affected which is evident through lower novel class performances for the relation distillation loss. Consequently, we find that the weighting can be used to tailor the desired plasticity and rigidity of an incremental model.

4) *Taxonomic Hierarchy and Hierarchical Loss*: We present the performance of different hierarchical loss functions in Tab. VI. The tree-min loss function significantly outperforms a simple hierarchical BCE loss where the logits of every leaf node v_L are multiplied with those of its ancestors (\mathcal{A}_{v_L}). Further, we note that the margin loss introduced in [32] does not result in a performance improvement with our incremental six-level deep hierarchy in hyperbolic space. We find that this geometric space already incorporates a favorable mapping of tree structures whose plasticity is negatively affected by the margin loss. Further, we ablate different taxonomy trees (shown in the supplementary material Sec. S.2) in Tab. VII. We observe a significant performance decrease of 12.97pp when formulating the incremental task with only three task levels. Consequently, we emphasize the benefit of deep hierarchies to prevent forgetting and acquire new knowledge.

TABLE VII: Influence of different class taxonomy trees (\mathcal{H}) for results on Cityscapes in mIoU (%).

\mathcal{H}	14-1 (6 tasks)		
	1-14	15-19	all
\mathcal{H}_3	60.86	32.57	50.75
\mathcal{H}_4	72.51	30.44	58.37
\mathcal{H}_6	73.03	42.47	61.74

TABLE VIII: Influence of different curvatures for results on Cityscapes in mIoU (%).

Curvature	14-1 (6 tasks)			
	1-14 ₀	1-14	15-19	all
0.1	74.42	71.82	42.24	60.84
1	72.48	72.96	38.33	60.66
2	74.85	73.03	42.47	61.74
5	74.59	73.17	37.39	60.57
10	74.77	72.93	35.56	59.94

5) *Curvature*: We observe the influence of different curvatures in Tab. VIII. While [26] report minor performance changes as an effect of this hyperparameter, we note that our CISS task is significantly influenced by it. While a lower curvature ($c = 0.1$) eases learning novel classes, the forgetting of base classes is more pronounced. Further, a high curvature ($c = 10$) results in worse performance for all classes. We reason this observation with the reduced size of the feature space.

E. Qualitative Results

We present qualitative evaluations of TOPICS with the best performing baseline on Cityscapes in Fig. 6a. We observe that both methods can precisely segment various classes e.g. pedestrians, cars, and vegetation. While DKD [21] tends to incorrectly classify flat surfaces as background in Fig. 6a (i, ii), our method superiorly remembers those old classes and continuously to accurately predict them after having learned new classes. This characteristic can be attributed to our strategy of maintaining knowledge by modeling the class hierarchy in hyperbolic space. Further, we note that DKD [21] merges objects with their respective background in Fig. 6a iii) and is not able to distinguish between the incremental classes 'rider' and 'pedestrian' which are learned sequentially. On the other hand, our method rarely confuses the named classes and maintains knowledge of all incremental classes. We reason this observation with our knowledge retention losses which ensures that

relevant relations are maintained when new classes are added.

On Mapillary Vistas v2.0, we observe that our approach and the best baseline can superiorly detect 'cars' and 'traffic lights' which are learned in the last two incremental steps as shown in Fig. 6b. However, while TOPICS is consistently able to identify the complete road structure, DKD [21] incorrectly predicts large shapes of other classes in Fig. 6b (i, iii, iv). We find that this behavior is hazardous in autonomous driving scenarios where misdetections lead to emergency braking. Both methods fail to predict markings and capture the complete shape of traffic signs in Fig. 6b (i) and Fig. 6b (iv).

V. CONCLUSION

We present TOPICS, a novel CISS approach that models features conforming to taxonomy-tree structures on the Poincaré ball to balance rigidity and plasticity in incremental learning. TOPICS further maintains implicit class relations between old class hyperplanes and constraints features to have equidistant radii. We presented extensive experimental evaluations of eight incremental settings on Cityscapes and Mapillary Vistas 2.0 that demonstrated that TOPICS achieves state-of-the-art performance. Our method is one of the early works that uniformly addresses the bifurcation of previously observed classes and incremental classes from the background. Further, we emphasize the benefit of hierarchical modeling in hyperbolic space and motivate future work to explore its potential for various open-world challenges.

ACKNOWLEDGEMENT

The authors thank Kshitij Sirohi for technical discussions.

REFERENCES

- [1] R. Mohan and A. Valada, "Perceiving the invisible: Proposal-free amodal panoptic segmentation," *IEEE Robotics and Automation Letters*, vol. 7, no. 4, pp. 9302–9309, 2022.
- [2] E. Greve, M. Büchner, N. Vödisch, W. Burgard, and A. Valada, "Collaborative dynamic 3d scene graphs for automated driving," *arXiv preprint arXiv:2309.06635*, 2023.
- [3] N. Gosala, K. Petek, P. L. Drews-Jr, W. Burgard, and A. Valada, "Skyeye: Self-supervised bird's-eye-view semantic mapping using monocular frontal view images," in *Proc. IEEE Conf. Comput. Vis. Pattern Recog.*, 2023, pp. 14 901–14 910.
- [4] M. Käppeler, K. Petek, N. Vödisch, W. Burgard, and A. Valada, "Few-shot panoptic segmentation with foundation models," *arXiv preprint arXiv:2309.10726*, 2023.
- [5] R. Mohan, K. Kumaraswamy, J. V. Hurtado, K. Petek, and A. Valada, "Panoptic out-of-distribution segmentation," *IEEE Robotics and Automation Letters*, 2024.
- [6] D.-W. Zhou, Q.-W. Wang, Z.-H. Qi, H.-J. Ye, D.-C. Zhan, and Z. Liu, "Deep class-incremental learning: A survey," *arXiv preprint arXiv:2302.03648*, 2023.
- [7] F. Cermelli, M. Cord, and A. Douillard, "Comformer: Continual learning in semantic and panoptic segmentation," *Proc. IEEE Conf. Comput. Vis. Pattern Recog.*, 2023.
- [8] F. Cermelli, M. Mancini, S. Rota Bulò, E. Ricci, and B. Caputo, "Modeling the background for incremental learning in semantic segmentation," in *Proc. IEEE Conf. Comput. Vis. Pattern Recog.*, 2020.
- [9] A. Douillard, Y. Chen, A. Dapogny, and M. Cord, "Plop: Learning without forgetting for continual semantic segmentation," *Proc. IEEE Conf. Comput. Vis. Pattern Recog.*, pp. 4039–4049, 2020.
- [10] Z. Zhang, G. Gao, Z. Fang, J. Jiao, and Y. Wei, "Mining unseen classes via regional objectness: A simple baseline for incremental segmentation," in *Adv. Neural Inform. Process. Syst.*, vol. 35, 2022, pp. 24 340–24 353.
- [11] S. Cha, b. kim, Y. Yoo, and T. Moon, "Ssul: Semantic segmentation with unknown label for exemplar-based class-incremental learning," in *Adv. Neural Inform. Process. Syst.*, vol. 34, 2021, pp. 10 919–10 930.
- [12] M. Cordts, M. Omran, S. Ramos, T. Rehfeld, M. Enzweiler, R. Benenson, U. Franke, S. Roth, and B. Schiele, "The cityscapes dataset for semantic urban scene understanding," in *Proc. IEEE Conf. Comput. Vis. Pattern Recog.*, 2016.
- [13] G. Neuhold, T. Ollmann, S. Rota Bulò, and P. Kotschieder, "The mapillary vistas dataset for semantic understanding of street scenes," in *Proc. Int. Conf. Comput. Vis.*, 2017, pp. 4990–4999.
- [14] A. Maracani, U. Michieli, M. Toldo, and P. Zanuttigh, "Recall: Replay-based continual learning in semantic segmentation," in *Proc. Int. Conf. Comput. Vis.*, 2021, pp. 7026–7035.
- [15] J. Chen, R. Cong, Y. LUO, H. Ip, and S. Kwong, "Saving 100x storage: Prototype replay for reconstructing training sample distribution in class-incremental semantic segmentation," in *Adv. Neural Inform. Process. Syst.*, 2023.
- [16] C.-B. Zhang, J.-W. Xiao, X. Liu, Y.-C. Chen, and M.-M. Cheng, "Representation compensation networks for continual semantic segmentation," in *Proc. IEEE Conf. Comput. Vis. Pattern Recog.*, 2022, pp. 7053–7064.
- [17] J.-W. Xiao, C.-B. Zhang, J. Feng, X. Liu, J. van de Weijer, and M.-M. Cheng, "Endpoints weight fusion for class incremental semantic segmentation," in *Proc. IEEE Conf. Comput. Vis. Pattern Recog.*, 2023, pp. 7204–7213.
- [18] D. Goswami, R. Schuster, J. van de Weijer, and D. Stricker, "Attribution-aware weight transfer: A warm-start initialization for class-incremental semantic segmentation," in *Proc. of the IEEE/CVF Winter Conf. on Applications of Comput. Vis.*, 2023, pp. 3195–3204.
- [19] Q. Wang, Y. Wu, L. Yang, W. Zuo, and Q. Hu, "Layer-specific knowledge distillation for class incremental semantic segmentation," *IEEE Trans. on Image Processing*, vol. 33, pp. 1977–1989, 2024.
- [20] Y. Qiu, Y. Shen, Z. Sun, Y. Zheng, X. Chang, W. Zheng, and R. Wang, "Sats: Self-attention transfer for continual semantic segmentation," *Pattern Recognition*, vol. 138, p. 109383, 2023.
- [21] D. Baek, Y. Oh, S. Lee, J. Lee, and B. Ham, "Decomposed knowledge distillation for class-incremental semantic segmentation," in *Adv. Neural Inform. Process. Syst.*, 2022.
- [22] C. Lang, A. Braun, L. Schillingmann, and A. Valada, "On hyperbolic embeddings in object detection," in *DAGM German Conference on Pattern Recognition*, 2022, pp. 462–476.
- [23] Y. Cui, Z. Yu, W. Peng, Q. Tian, and L. Liu, "Rethinking few-shot class-incremental learning with open-set hypothesis in hyperbolic geometry," *IEEE Trans. on Multimedia*, 2023.
- [24] O. Ganea, G. Bécigneul, and T. Hofmann, "Hyperbolic neural networks," *Adv. Neural Inform. Process. Syst.*, vol. 31, 2018.
- [25] K. Desai, M. Nickel, T. Rajpurohit, J. Johnson, and R. Vedantam, "Hyperbolic Image-Text Representations," in *Proc. of the Int. Conf. on Machine Learning*, 2023.
- [26] M. G. Atigh, J. Schoep, E. Acar, N. Van Noord, and P. Mettes, "Hyperbolic image segmentation," in *Proc. IEEE Conf. Comput. Vis. Pattern Recog.*, 2022, pp. 4453–4462.
- [27] S. Xu, Y. Sun, F. Zhang, A. Xu, X.-S. Wei, and Y. Yang, "Hyperbolic space with hierarchical margin boosts fine-grained learning from coarse labels," in *Adv. Neural Inform. Process. Syst.*, 2023.
- [28] M. van Spengler, E. Berkhout, and P. Mettes, "Poincaré resnet," *Proc. Int. Conf. Comput. Vis.*, pp. 5396–5405, 2023.
- [29] S. Weber, B. Zöngür, N. Araslanov, and D. Cremers, "Flattening the parent bias: Hierarchical semantic segmentation in the poincaré ball," in *Proc. IEEE Conf. Comput. Vis. Pattern Recog.*, 2024.
- [30] L. Franco, P. Mandica, K. Kallidromitis, D. Guillory, Y.-T. Li, T. Darrell, and F. Galasso, "Hyperbolic active learning for semantic segmentation under domain shift," *arXiv preprint arXiv:2306.11180*, 2024.
- [31] Y. Chen, Z. Li, Z. Hu, and N. Vasconcelos, "Taxonomic class incremental learning," *arXiv preprint arXiv:2304.05547*, 2023.
- [32] L. Li, W. Wang, T. Zhou, R. Quan, and Y. Yang, "Semantic hierarchy-aware segmentation," *IEEE Trans. Pattern Anal. Mach. Intell.*, vol. 46, no. 4, pp. 2123–2138, 2024.
- [33] Z. Lin, D. Pathak, Y.-X. Wang, D. Ramanan, and S. Kong, "Continual learning with evolving class ontologies," *Adv. Neural Inform. Process. Syst.*, vol. 35, pp. 7671–7684, 2022.
- [34] S. Li, X. Ning, S. Zhang, L. Guo, T. Zhao, H. Yang, and Y. Wang, "Tep: Triplet contrastive-relationship preserving for class-incremental learning," in *Proc. of the IEEE/CVF Winter Conf. on Applications of Comput. Vis.*, 2024, pp. 2031–2040.
- [35] M. Kochurov, R. Karimov, and S. Kozlukov, "Geoopt: Riemannian optimization in pytorch," *arXiv preprint arXiv:2005.02819*, 2020.
- [36] S. Mittal, S. Galesso, and T. Brox, "Essentials for class incremental learning," in *Proc. of the IEEE/CVF Conf. on Comput. Vis. and Pattern Recog. Workshops*, 2021, pp. 3513–3522.

Taxonomy-Aware Continual Semantic Segmentation in Hyperbolic Spaces for Open-World Perception

- Supplementary Material -

Julia Hindel, Daniele Cattaneo and Abhinav Valada

In this supplementary material, we present extended results on Cityscapes and Mapillary Vistas 2.0 in Sec. S.1. Further, we show additional illustrations of the applied taxonomic trees in Sec. S.2.

S.1. EXTENDED QUANTITATIVE RESULTS

We perform a detailed analysis of the base IoU scores shown in Sec. IV-C. All compared methods achieve different performances after base training which significantly influences the observed performance on base classes after the final incremental step. Consequently, we note the relative performance degradation of base classes as a percentage of their initial performance in Tab. S.1 and Tab. S.2. On Cityscapes, we observe that TOPICS presents the least relative performance drop on incremental settings from the background. For the incremental setting from known classes, baseline methods such as DKD [21] and MicroSeg [10] can similarly retain knowledge on the non-incremented base class 'sky' which we reason with their missing plasticity to generalize to novel classes.

We show in Tab. S.2 that TOPICS has the lowest relative performance degradation on base classes in three scenarios. Consequently, we reason that DKD [21] achieves the highest absolute IoU on base classes for this dataset as a result of its favorable performance during the initial base training. We highlight that lower relative performance degradation represents true knowledge retention capabilities which is the focus of this work. Further, we believe that a stronger model can resolve this problem and highlight that TOPICS can be readily employed with different backbones.

S.2. EXTENDED QUANTITATIVE RESULTS

In this section, we present visualizations of different taxonomic trees for Cityscapes and Mapillary Vista 2.0. In Fig. S.1 and Fig. S.4, we show the taxonomic trees used in Sec. IV-C. Further, we present smaller taxonomic trees in Fig. S.2 and Fig. S.3. Their respective results are presented in Sec. IV-D.4.

TABLE S.1: Continual semantic segmentation results on Cityscapes in mIoU (%). Tasks defined as $\mathcal{C}^1\text{-}\mathcal{C}^T(T)$ tasks and h class hierarchy increments. The relative decrease in performance on \mathcal{C}^1 is recorded in (%).

Method	14-1 (6 tasks)			10-1 (10 tasks)			7-4 (4 tasks)h			7-18 (2 tasks)h		
	1-14	↓1-14 ₀ [%]	all	1-10	↓1-10 ₀ [%]	all	1-7	↓1-7 ₀ [%]	all	1-7	↓1-7 ₀ [%]	all
PLOP [9]	63.54	3.64	48.33	60.75	5.43	42.96	88.56	1.25	20.75	88.73	1.07	17.99
MiB [8]	66.37	5.75	50.05	61.80	9.80	45.73	77.66	13.0	9.83	90.10	0.0	9.64
MiB + AWT [18]	65.60	6.84	50.72	60.97	11.07	46.55	84.65	5.16	13.64	90.19	0.0	9.56
DKD [21]	68.83	3.21	51.86	66.77	4.51	48.92	89.46	0.0	4.98	89.19	0.1	8.32
MicroSeg [10]	51.35	8.86	38.84	44.37	15.73	32.78	86.39	0.0	5.79	86.37	0.0	11.26
TOPICS (Ours)	73.03	2.43	61.74	71.37	1.99	59.36	90.02	0.5	50.69	90.33	0.2	59.98

TABLE S.2: Continual semantic segmentation results on Mapillary Vistas 2.0 in mIoU (%). Tasks defined as $\mathcal{C}^1\text{-}\mathcal{C}^T(T)$ tasks and h class hierarchy increments. The relative decrease in performance on \mathcal{C}^1 is recorded in (%).

Method	51-30 (3 tasks)			71-10 (5 tasks)			39-84 (2 tasks)h			39-21 (5 tasks)h		
	1-51	↓1-51 ₀ [%]	all	1-71	↓1-71 ₀ [%]	all	1-39	↓1-39 ₀ [%]	all	1-39	↓1-39 ₀ [%]	all
PLOP [9]	20.83	17.96	14.59	18.12	27.17	13.83	19.15	44.38	9.51	17.79	77.37	6.64
MiB [8]	16.72	34.15	13.77	15.10	39.31	12.58	19.38	43.71	11.64	16.49	52.11	8.86
MiB + AWT [18]	18.33	27.81	15.89	15.78	36.58	13.91	19.76	42.61	15.47	17.75	48.45	12.84
DKD [21]	25.49	22.48	18.74	22.71	19.27	18.65	24.24	36.69	9.15	28.04	26.77	8.06
MicroSeg [10]	9.39	28.54	6.62	8.38	36.71	6.65	12.70	42.92	4.41	13.69	38.47	4.08
TOPICS (Ours)	23.76	18.88	20.35	22.10	16.54	19.20	24.16	32.94	21.94	26.67	25.98	23.35

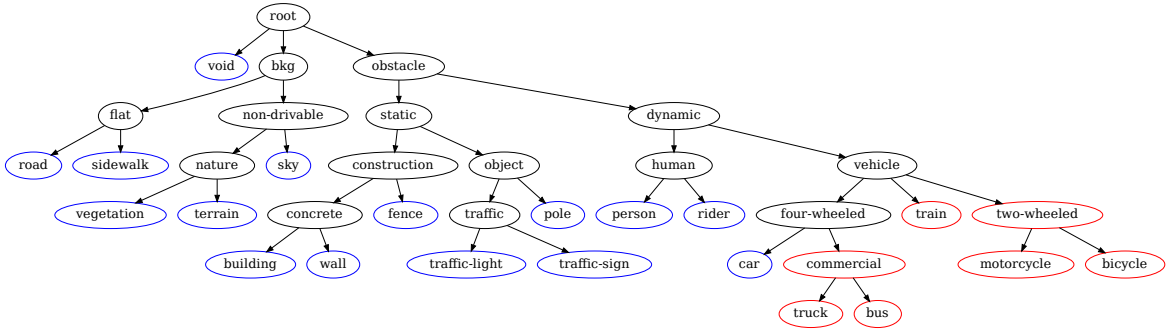


Fig. S.1: Visualization of the Cityscapes class taxonomic tree \mathcal{H}_6 . Base classes (\mathcal{C}^1) are colored in black (ancestors) and blue (leaf classes) whereas novel classes ($\mathcal{C}^{2:T}$) are colored in red.

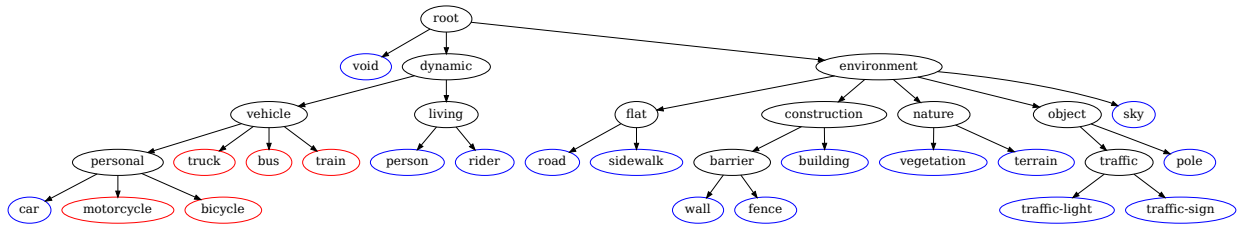


Fig. S.2: Visualization of the Cityscapes class taxonomic tree \mathcal{H}_4 . Base classes (\mathcal{C}^1) are colored in black (ancestors) and blue (leaf classes) whereas novel classes ($\mathcal{C}^{2:T}$) are colored in red for Cityscapes 15-1(6 tasks).

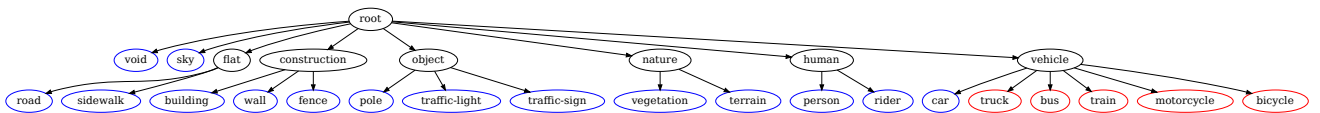


Fig. S.3: Visualization of the Cityscapes class taxonomic tree \mathcal{H}_3 . Base classes (\mathcal{C}^1) are colored in black (ancestors) and blue (leaf classes) whereas novel classes ($\mathcal{C}^{2:T}$) are colored in red for Cityscapes 15-1(6 tasks).

